공학석사학위논문

결합된 쿼드로터 무인비행로봇의 모델링 및 제어

Modeling and Control of Asymmetrically Coupled Quadrotor UAVs

2015 년 2 월

서울대학교 대학원

기계항공공학부

최 병 화

결합된 쿼드로터 무인비행로봇의 모델링 및 제어

Modeling and Control of Asymmetrically Coupled Quadrotor UAVs

지도교수 이 동 준

이 논문을 공학석사 학위논문으로 제출함

2015 년 2 월

서울대학교 대학원

기계항공공학부

최 병 화

최병화의 공학석사 학위논문을 인준함

2015 년 2 월

위 원 장 _____

부위원장 _____

위 원 _____

Abstract

Modeling and Control of Asymmetrically Coupled Quadrotor UAVs

Francis Byonghwa Choi
Mechanical & Aerospace Engineering
The Graduate School
Seoul National University

In this thesis, we introduce a novel concept of asymmetrically coupled quadrotor UAVs (Unmanned Aerial Vehicles) system. The proposed system is composed with two quadrotor UAVs that are asymmetrically coupled with each other. This coupled system has advantages in the sense of overcoming under-actuation and payload problems compared to single conventional quadrotor UAV. That is, the proposed system has 5 actuation DOFs while single quadrotor UAV has 4 actuation DOFs, where the additional actuation can be exploited for decoupling translation and rotation in a certain direction. This feature increases the versatility and is useful for real tasks such as aerial tool operation. We first model the coupled quadrotor system and design a controller which is based on the backstepping control and optimization to guarantee positiveness of thrusts. Simulation results are presented to validate the theory and to demonstrate the advantages of the proposed system.

Keywords: Quadrotor UAV, Backstepping control, Under-actuation
Student Number: *2013-20721*

Contents

List of Figures v

List of Tables vii

Abbreviations viii

Physical Constants ix

Symbols x

1 Introduction 1

1.1 Motivation and Objectives 1

1.2 State of the Art 3

1.3 Contribution of this Work 4

2 System Modeling 6

2.1 Asymmetrically Coupled Quadrotor UAVs 6

2.2 Dynamics of Asymmetrically Coupled Quadrotor UAVs 9

2.3 Thrust Relationship 13

3 Control Design 16

3.1 Backstepping Control 17
3.2 Positive Thrust Constraint 23

4 Simulation **26**
4.1 Simulation Scheme 26
4.2 Simulation Results 28
4.2.1 Trajectory tracking 29
4.2.2 Translation along x-axis without rotation 31
4.2.3 Rotation without translation 35
4.2.4 Combination case 37
4.2.5 Tool operation example 40

5 Conclusion and Future Work **44**
5.1 Conclusion 44
5.2 Future Work 45

List of Figures

2.1 3-D CAD concept design of asymmetrically coupled quadrotor UAVs 7
2.2 Thrust vectoring examples 8
2.3 3-D modeling of the system with designation of axes and the order of thrust forces 10
2.4 2-D modeling view of the system with designation of frames . . . 11

3.1 Positiveness of thrust 24

4.1 Simulation structure 27
4.2 Trajectory tracking plot for circular trajectory 29
4.3 Position error plot for circular trajectory 30
4.4 Angular velocity plot for circular trajectory 30
4.5 Thrust force plot for circular trajectory 31
4.6 Simulation snapshot for x-axis trajectory 32
4.7 Trajectory tracking plot for x-axis trajectory 33
4.8 Angular velocity plot for x-axis trajectory 33
4.9 Thrust force plot for x-axis trajectory 34
4.10 Simulation snapshot for rotation at set-point 35
4.11 Angular velocity plot for rotation at set-point 36
4.12 Keeping set-point position (0, 0, -1) while rotating 36
4.13 Thrust force plot for rotation at set-point 37
4.14 Trajectory tracking plot for combination case 38
4.15 Position error plot for combination case 38
4.16 Angular velocity plot for combination case 39

4.17 Thrust force plot for combination case 39
4.18 Simulation snapshot for tool operation 41
4.19 Trajectory tracking plot $x \rightarrow x_r$ for tool operation 42
4.20 Difference between desired trajectory x_d and reference trajectory x_r along contact 42
4.21 Thrust force plot for tool operation 43

5.1 Concept design of modular quadrotor UAVs system 46

List of Tables

4.1 Parameters/gains used in simulation 28

Abbreviations

UAV	**U**nmanned **A**erial **V**ehicle
VTOL	**V**ertical **T**ake-**O**ff and **L**anding
DOF	**D**egree **O**f **F**reedom
NED	**N**orth **E**ast **D**own
OpenGL	**Open** source **G**raphics **L**ibrary

Physical Constants

Standard gravity $g = 9.806\ 65\ \mathrm{m/s^2}$ (exact)

Symbols

$\{\mathcal{O}\}$	Earth (inertial) frame	
$\{\mathcal{B}_{1,2}\}$	Body-fixed frame of each quadrotor UAV	
$\{\mathcal{C}\}$	CoM frame of asymmetrically coupled quadrotor UAVs	
x ($\dot{x}$, $\ddot{x}$)	Position (velocity, acceleration) of $\{\mathcal{C}\}$ relative to $\{\mathcal{O}\}$	m (m/s, m/s^2)
R_c	Rotation matrix of $\{\mathcal{C}\}$ w.r.t $\{\mathcal{O}\}$	$\in SO(3)$
$R_{1,2}$	Rotation matrix of $\{\mathcal{B}_{1,2}\}$ w.r.t $\{\mathcal{O}\}$	$\in SO(3)$
ϕ, θ, ψ	Roll, pitch, yaw angle	rad
ω	Body-fixed angular velocity	rad/s
$\lambda_{1,2}$	Total thrust of each quadrotor UAV	N
$\tau_{\phi,\theta,\psi}$	Total torque of coupled system	N·m
α	Coupling angle	rad

Chapter 1

Introduction

1.1 Motivation and Objectives

Followed by the development of miniaturized sensors, actuators, and materials, and advancement in performance of microprocessors resulted in great interest in micro Unmanned Aerial Vehicles (UAV) over the last decades. Especially quadrotor UAV has been one of the most popular platform due to its simple and symmetric structure so that control is quite easy and stable. Also, Vertical Take-off and Landing (VTOL) and hovering abilities are useful for various tasks along with capability of agile and fast flight maneuver. [1–5] There have been numerous works related to quadrotor UAV but most of them were focused on flight maneuver of it. Therefore, quadrotor UAV has been mostly used for *passive*

tasks, e.g. reconnaissance, surveillance, transportation, and aerial photography, etc. Recently, using quadrotor UAV platform not only for passive tasks, but for *active* tasks such as tool operation or aerial manipulation is becoming hot research topic. [6–9]

Single conventional quadrotor UAV, however, has inherent under-actuation problem, that is, quadrotor UAV has 4 actuations for 6 degree-of-freedoms (DOFs) of motion, thus translation and rotation are coupled. This becomes a huge limitation for doing a manipulation tasks. Aerial tool operation, for example, is usually done by combining a rigid tool over/under a quadrotor UAV to do specific missions. But due to under-actuation, whenever quadrotor UAV moves, the platform itself should be tilted which induces undesired motion of end-effector. This raises difficult control problems. [6] Also, due to insufficient battery performance, low payload is another limitation of single quadrotor UAV.

For the above reasons, our research objective in this thesis is to build a novel design concept of UAV to overcome the limitations of single conventional quadrotor UAV, i.e. under-actuation and low payload problem. Also, we want to build not just a single vehicle, but a integrated system that can be used for various applications and has high flexibility. Therefore, we design the asymmetrically coupled quadrotor UAVs system which is composed with two conventional quadrotor UAVs. Combining two quadrotor UAVs with non-zero coupling angle creates additional actuation so that the system becomes more versatile. Also, it is no wonder that two quadrotor UAVs system will have more payload capacity. Our

final goal is to extend this idea to modular quadrotor UAVs system. Modular system has many advantages like easy extension and flexible to any given condition, to name a few. [10, 11] If an user needs more payload, then he/she can just combine more modules to adjust to the mission. As a first step of the whole story, here in this thesis, we consider the system composed with two quadrotor UAVs that are rigidly connected to each other asymmetrically, so called *asymmetrically coupled quadrotor UAVs*.

1.2 State of the Art

As the quadrotor UAV gets more attention, many researchers have worked with it over the last years. In the beginning, most of them were focused on the flight control of a quadrotor UAV. [4, 5, 12–14] Soon they started to find useful applications of quadrotor UAV, such as cable-suspended transportation [15], aerial contruction [16], aerial tool operation [6], aerial manipulation [7, 17], and so on.

Single quadrotor UAV, however, has limitations in two senses: under-actuation and low payload. These limitations make the system complex to control and act as huge obstacle for using it in real tasks. For this, there have been many researchers to overcome these problems by modifying the design [18–22], using multiple UAVs [8, 9, 23], or both [24, 25]. In [18–20], they introduced a quadrotor UAV with tilting propellers so that overcoming under-actuation. But as they added servo motors to the system, the control is too much complicated and there

is no improvement on payload. In [21, 22], they built a variable-pitch quadrotor UAV which can change the pitch angle of the propellers so that can change the thrust direction upside down. But this system is still under-actuated and has no advantage doing useful assignments. On the other hand, there are a number of researches on using multiple UAVs to overcome low payload problem. In [23], the author suggested a control framework for multiple UAVs, but it is only for flight maneuver so not much useful for real tasks. In [8, 9], they developed cable-suspended/grasping cooperative transportation system using multiple quadrotor UAVs, yet, the system is quite complicated and the application is limited to transportation. Also in [24], the authors introduced a novel system that is modular aerial vehicle which can joint/disjoint in any configurations. This system is seemingly awesome, however it has no advantage in actuation DOF and is not applicable for real assignments. In [25], which is fairly close to our system, they developed a vehicle that two ducted-fan is rigidly attached each other. However, ducted-fan is not a popular platform than quadrotor UAV and they have no consideration on modularizing, joint/disjoint ability, and expanding to unlimited number of UAVs.

1.3 Contribution of this Work

In this paper, to overcome limitations of single conventional quadrotor, we introduce a novel system that two quadrotors combined each other asymmetrically. This system has advantages in actuation DOFs as well as payload. In the sense of

actuation DOFs, asymmetrically coupled quadrotor system can decouple translation and rotation in certain direction (e.g. x-axis in this thesis) while single quadrotor can't. Exploiting this feature, the proposed system has increased versatility of behaviors, thus expecting to be useful for useful tasks like tool operation. The ultimate goal of this research is to build a system that the modular quadrotors can attach/detach to nearby others in any user-intended configurations.

The rest of this paper is structured as follows. In Sec. 2, we first breifly introduce the asymmetrically coupled quadrotor UAVs and model the dynamics of the system, also defining the thrust relationship. We design backstepping controller and appropriate optimization for positive thrust constraint in Sec. 3. Then, Sec. 4 shows the simulation results to validate proposed system and controller and to reveal its features. Finally, some concluding remarks are given in Sec. 5.

Chapter 2

System Modeling

2.1 Asymmetrically Coupled Quadrotor UAVs

Single quadrotor UAV is an under-actuated system with 4 actuations for 6 DOFs motion, i.e. only 3-D translation and yawing motion are possible. Thrust direction is fixed to the z-axis of the body frame, thus it is indispensable to tilt itself to move in x- or y-axis. This is not a big demerit in pure flight maneuvers, but when using quadrotor UAV as a tool or manipulator platform it becomes huge obstacle, e.g. generation of undesired motion of end-effector. [6]

To overcome the limitation of single quadrotor UAV, we introduce a novel design concept of asymmetrically coupled quadrotor UAVs system where Fig. 2.1 shows the concept sketch of the system. As shown in the figure, two conventioanl

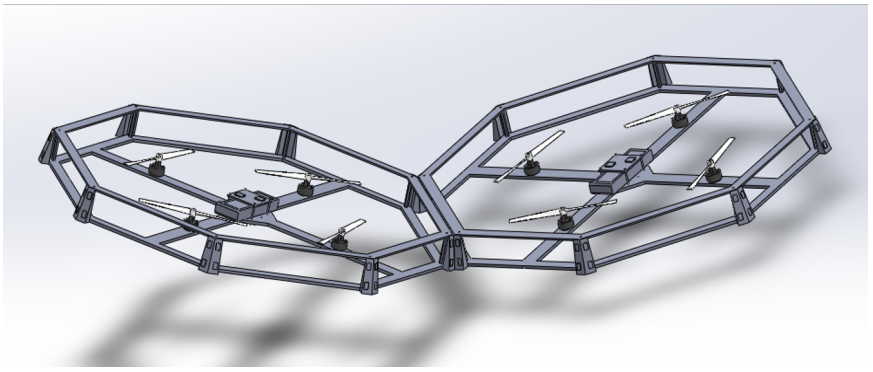

FIGURE 2.1: 3-D CAD concept design of asymmetrically coupled quadrotor UAVs

quadrotor UAVs are combined with non-zero coupling angle so that they compose an asymmetric system. From this feature, 2-D thrust vectoring is possible, that is, the net thrust can be controlled by the combination of two thrusts from each quadrotor UAV.

For easier understanding, Fig. 2.2 shows some examples of thrust vectoring. In (a), two thrusts from each quadrotor UAV are equal so that net thrust is standing on z-axis resulting in normal hovering flight. If one thrust, however, gets bigger than the other, net thrust is no longer parallel with z-axis and contains horizontal force component as in (b). This is what we call *2-D thrust vectoring*. This allows the system to translate without tilting which is impossible in single quadrotor UAV system. On the other hand, with this thrust vectoring capability, hovering in stationary position while tilting or changing the rotation attitude is

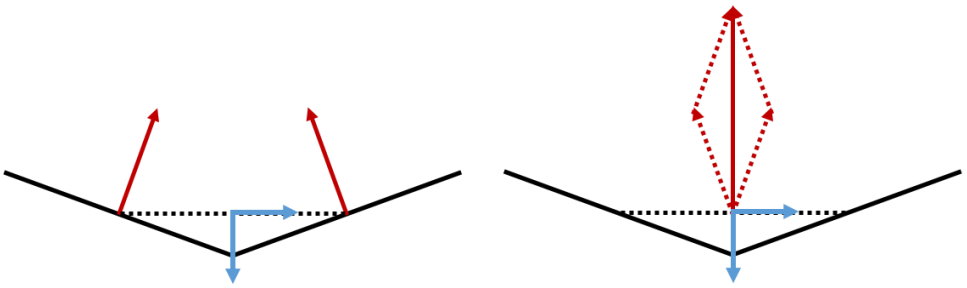

(a) Normal hovering case

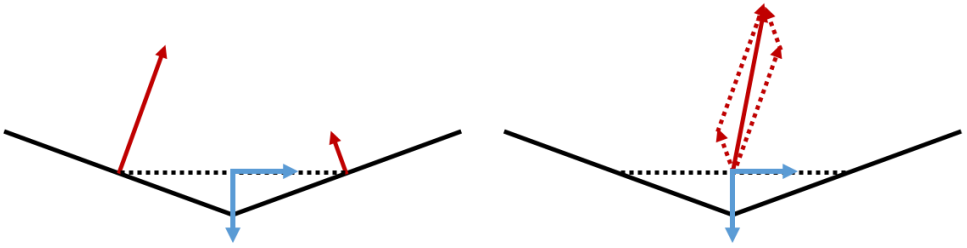

(b) Generating horizontal force

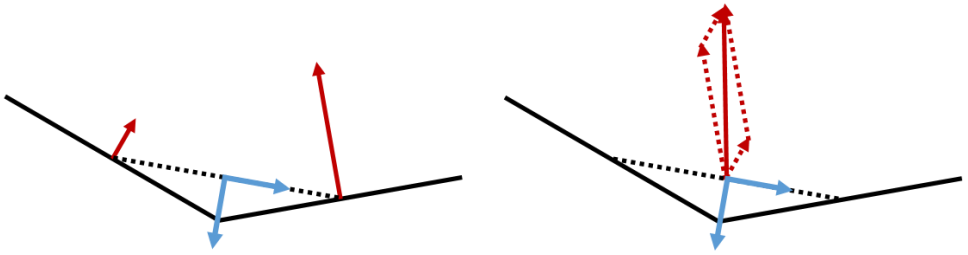

(c) Hovering while tilting

FIGURE 2.2: Thrust vectoring examples

also possible as in (c). Moreover, not only (b) and (c) case, but combination of them are possible, that is controlling translational motion and rotational behavior independently. This shows that the asymmetrically coupled quadrotor UAVs system can decouple translation and rotation in a certain direction, which is indeed coupled axis. The advantages of this feature will be demonstrated in Sec. 4 with various scenarios.

2.2 Dynamics of Asymmetrically Coupled Quadrotor UAVs

We first model the asymmetrically coupled quadrotor UAVs system as Fig. 2.3 and Fig. 2.4. Here, each quadrotor is same with conventional commercially available quadrotor UAV, however combined each other with coupling angle α as indicated in the figures.

According to the modeling, we can write translational and attitude dynamics similar to [5, 13, 26] as below:

$$m\ddot{x} = -\lambda_1 R_1 e_3 - \lambda_2 R_2 e_3 + mge_3 \tag{2.1}$$

$$J\dot{w} + w \times Jw = \tau \tag{2.2}$$

$$\dot{R}_c = R_c S(w) \tag{2.3}$$

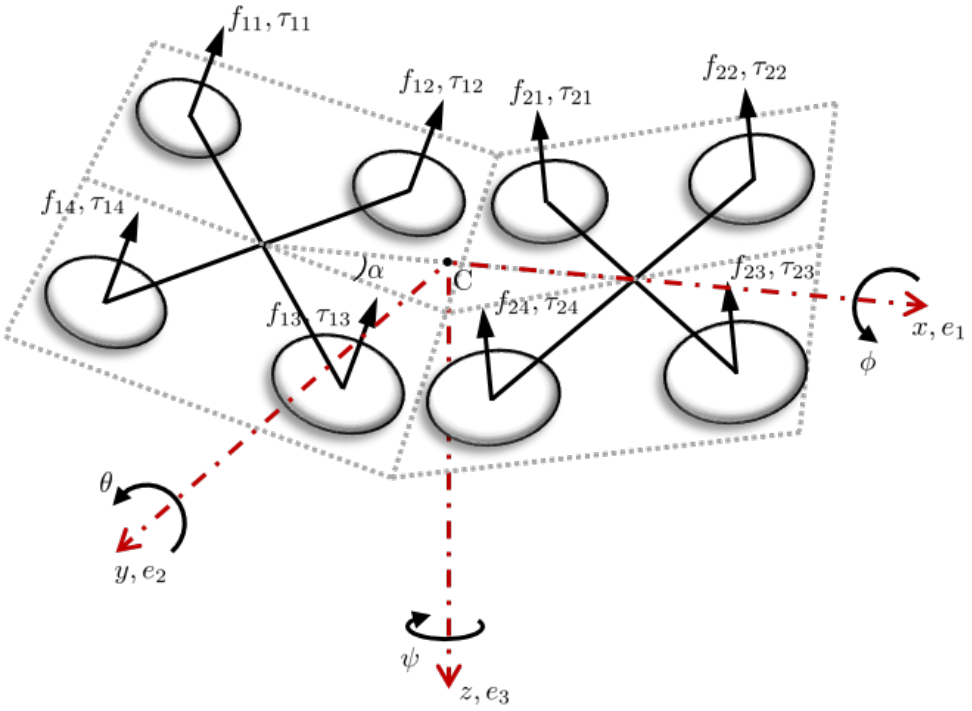

FIGURE 2.3: 3-D modeling of the system with designation of axes and the order of thrust forces

where $m > 0$ is the mass of coupled system, $x \in \Re^3$ is the Cartesian position of the center of mass w.r.t. the NED (north-east-down) Earth frame $\{\mathcal{O}\}$ with e_3 representing its down-direction, $\lambda_{1,2} \in \Re$ is the thrust of each quadrotor along the body-frame z-direction, $R_{1,2,c} \in SO(3)$ is the rotational matrix describing the body NED frame of each quadrotor and center of mass, respectively, w.r.t. the Earth frame, and $g = 9.80665 m/s^2$ is standard gravity. Also, $J \in \Re^{3\times3}$ is the inertia matrix w.r.t. the body frame, $w := [w_1, w_2, w_3]^T \in \Re^3$ is the angular

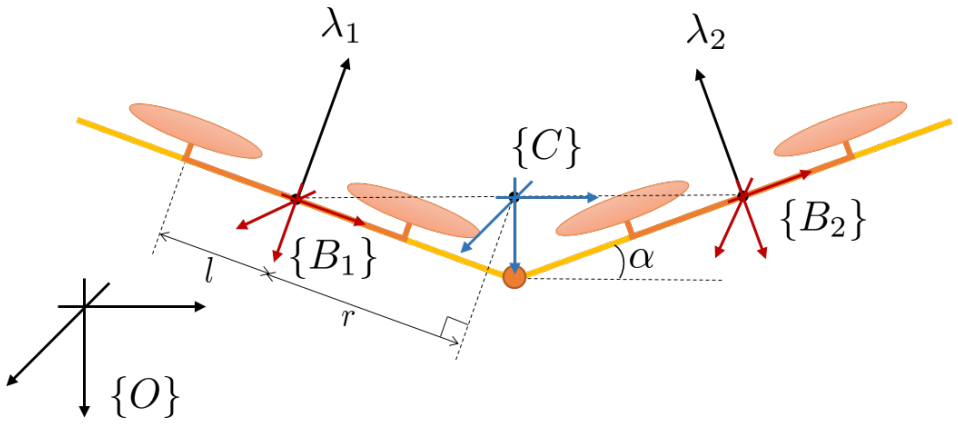

FIGURE 2.4: 2-D modeling view of the system with designation of frames

velocities of the body frame relative to the Earth frame expressed in the body frame, $\tau \in \Re^3$ is the torque input, and $S(\star) : \Re^3 \to so(3)$ is the skew-symmetric operator defined s.t. for $a, b \in \Re^3$, $S(a)b = a \times b$.

Since coupling angle α is constant and two quadrotors are connected in a certain direction (x-axis in this thesis), rotational matrices of each quadrotor have relationship between the rotational matrix of center-of-mass frame as below.

$$R_1 = R_c^o R_1^c = R_c R_{e_2}(-\alpha) \tag{2.4}$$

$$R_2 = R_c^o R_2^c = R_c R_{e_2}(\alpha) \tag{2.5}$$

where

$$R_{e_2}(\star) = \begin{bmatrix} \cos\star & 0 & \sin\star \\ 0 & 1 & 0 \\ -\sin\star & 0 & \cos\star \end{bmatrix}$$

representing the rotation around y-axis.

Using (2.4) and (2.5), translational dynamics (2.1) can be rewritten in the following simplified form

$$\begin{aligned} m\ddot{x} &= R_c \left[\begin{pmatrix} \lambda_1 \sin\alpha \\ 0 \\ -\lambda_1 \cos\alpha \end{pmatrix} + \begin{pmatrix} -\lambda_2 \sin\alpha \\ 0 \\ -\lambda_2 \cos\alpha \end{pmatrix} \right] + mge_3 \\ &= R_c \begin{bmatrix} (\lambda_1 - \lambda_2)\sin\alpha \\ 0 \\ -(\lambda_1 + \lambda_2)\cos\alpha \end{bmatrix} + mge_3 \end{aligned} \tag{2.6}$$

Note that this dynamics (2.6) is quite similar with that of single quadrotor UAV [5, 13, 26], but there are some more terms other than e_3 terms. This is from increased actuation DOFs ($4 \rightarrow 5$ actuations) and will be exploited in the control.

2.3 Thrust Relationship

Also, we can define the relationship between the control input (i.e. total thrust and the torque of coupled system) and individual thrust force from 8 rotors. Analysing the kinematic structure of the system, we can find relationship as below.

$$\Lambda := \begin{pmatrix} \lambda_1 \\ \lambda_2 \\ \tau_\phi \\ \tau_\theta \\ \tau_\psi \end{pmatrix} = \Sigma_\alpha \mathbf{f}_{ij} \tag{2.7}$$

where $\Lambda \in \Re^5$ is defined as control input, $\mathbf{f}_{ij} := [f_{11}, f_{12}, f_{13}, f_{14}, f_{21}, f_{22}, f_{23}, f_{24}]^T$ is thrust force vector shown in Fig. 2.3, and

$$\Sigma_\alpha = \begin{bmatrix} 1 & 1 & 1 & 1 & 0 & 0 & 0 & 0 \\ 0 & 0 & 0 & 0 & 1 & 1 & 1 & 1 \\ \sigma_1 - \sigma_2 & \sigma_1 + \sigma_2 & -\sigma_1 - \sigma_2 & -\sigma_1 + \sigma_2 & \sigma_1 + \sigma_2 & \sigma_1 - \sigma_2 & -\sigma_1 + \sigma_2 & -\sigma_1 - \sigma_2 \\ -\sigma_3 & \sigma_4 & \sigma_4 & -\sigma_3 & -\sigma_4 & \sigma_3 & \sigma_3 & -\sigma_4 \\ \sigma_5 + \sigma_6 & \sigma_5 - \sigma_6 & -\sigma_5 + \sigma_6 & -\sigma_5 - \sigma_6 & -\sigma_5 + \sigma_6 & -\sigma_5 - \sigma_6 & \sigma_5 + \sigma_6 & \sigma_5 - \sigma_6 \end{bmatrix}$$

with

$$\begin{aligned} \sigma_1 &= l\cos\alpha\ , & \sigma_2 &= k_\tau \sin\alpha \\ \sigma_3 &= l + r\ , & \sigma_4 &= l - r \\ \sigma_5 &= l\sin\alpha\ , & \sigma_6 &= k_\tau \cos\alpha \end{aligned}$$

where l, r are system parameters indicated in Fig. 2.4 and $k_\tau \in \Re$ is constant coefficient satisfying

$$\tau_{ij} = k_\tau f_{ij} \tag{2.8}$$

It is known that both thrust and torque generated from the rotor are proportional to the square of the rotation speed (i.e. $f \propto \Omega^2$ and $\tau \propto \Omega^2$), so we can write the relationship between thrust and torque as (2.8).

Since control input Λ has 5 DOFs while motion can be 6 DOFs (e.g. x, y, z-axis translation/rotation, respectively), the asymmetrically coupled quadrotor UAVs

system is still under-actuated. This system, however, earns 1 more DOF than single quadrotor so that can generate various interesting behaviors and will be described hereafter. But first, we design a controller for trajectory tracking and exploiting the system's features in Sec. 3.

Chapter 3

Control Design

In this chapter, we design a controller of asymmetrically coupled quadrotor UAVs system for trajectory tracking while satisfying the positive thrust constraint. To deal with this problem, we first consider the trajectory tracking matter of under-actuated (i.e. 5 actuations for 6 DOFs motion) system, and then design appropriate optimization for the constraint of positiveness of thrust forces. Extension for real useful tasks like tool operation is not that much different to trajectory tracking, rather similar to [6]. The work presented here is a first step for utilizing the asymmetrically coupled multiple modular quadrotor UAVs system for aerial tool operation or aerial manipulation which will be future research topic.

3.1 Backstepping Control

For the trajectory tracking control of the asymmetrically coupled quadrotor UAVs system, we first design control u_d as below.

$$m\ddot{x} = u_d := m\ddot{x}_d - b(\dot{x} - \dot{x}_d) - k(x - x_d) \tag{3.1}$$

where $x_d, \dot{x}_d, \ddot{x}_d$ are desired position, velocity, and accleration, respectively, and $b, k > 0$ are constant gains. Then the closed-loop dynamics can be written as

$$\begin{aligned} m\ddot{e} + b\dot{e} + ke &= R_c \begin{bmatrix} (\lambda_1 - \lambda_2)\sin\alpha \\ 0 \\ -(\lambda_1 + \lambda_2)\cos\alpha \end{bmatrix} + mge_3 - u_d \\ &=: \nu \end{aligned} \tag{3.2}$$

where $e := x - x_d$ is the position error. Here, we define $\nu \in \Re^3$ as a *control generation error* which is induced by the under-actuation of the system. Thus, if we can make ν to be zero then all the error terms will converge to origin [27]. For the sake of eliminating ν, similar to [5, 26, 28], we first design Lyapunov candidate function as follows.

$$V_1 = \frac{1}{2}\begin{pmatrix}\dot{e}\\ e\end{pmatrix}^T \begin{bmatrix} m & \epsilon m \\ \epsilon m & k+\epsilon b \end{bmatrix} \begin{pmatrix}\dot{e}\\ e\end{pmatrix} \tag{3.3}$$

where $\epsilon > 0$ is a constant to be decided below. Differentiating this V_1 with (3.2), we get

$$\dot{V}_1 = -\begin{pmatrix}\dot{e}\\ e\end{pmatrix}^T \begin{bmatrix} b-\epsilon m & 0 \\ 0 & \epsilon k \end{bmatrix} \begin{pmatrix}\dot{e}\\ e\end{pmatrix} + (\dot{e}+\epsilon e)^T \nu \tag{3.4}$$

If $\nu = 0$ in (3.4), we would have $(\dot{e}, e) \to 0$ exponentially. To address this term, we design a new Lyapunov function augmented with (3.3) as

$$V = V_1 + \frac{1}{2\gamma}\nu^T\nu \tag{3.5}$$

where $\gamma > 0$ is a constant gain. Differentiating (3.5), then we have

$$\dot{V} = -\begin{pmatrix}\dot{e}\\ e\end{pmatrix}^T \begin{bmatrix} b-\epsilon m & 0 \\ 0 & \epsilon k \end{bmatrix} \begin{pmatrix}\dot{e}\\ e\end{pmatrix} + (\dot{e}+\epsilon e)^T \nu + \frac{1}{\gamma}\nu^T\dot{\nu} \tag{3.6}$$

which suggests the backstepping update law for $\dot{\nu}$ to be determined as

$$\dot{\nu} = -\gamma(\dot{e}+\epsilon e) - \eta\nu \tag{3.7}$$

resulting in, with constant $\eta > 0$,

$$\dot{V} = -\begin{pmatrix} \dot{e} \\ e \end{pmatrix}^T \begin{bmatrix} b - \epsilon m & 0 \\ 0 & \epsilon k \end{bmatrix} \begin{pmatrix} \dot{e} \\ e \end{pmatrix} - \frac{\eta}{\gamma} \nu^T \nu \tag{3.8}$$

Consequently, we can guarantee that $(\dot{e}, e, \nu) \to 0$ if we choose $0 < \epsilon < \frac{b}{m}$ and $\eta, \gamma > 0$.

Now, we need to decode the backstepping update law (3.7). Differentiating (3.2), with (3.7),

$$\begin{aligned} & R_c \begin{bmatrix} (\dot{\lambda}_1 - \dot{\lambda}_2)\sin\alpha \\ 0 \\ -(\dot{\lambda}_1 + \dot{\lambda}_2)\cos\alpha \end{bmatrix} + R_c S(w) \begin{bmatrix} (\lambda_1 - \lambda_2)\sin\alpha \\ 0 \\ -(\lambda_1 + \lambda_2)\cos\alpha \end{bmatrix} \\ & - \dot{u}_d = -\gamma(\dot{e} + \epsilon e) - \eta\nu \end{aligned} \tag{3.9}$$

Reorganizing (3.9), we get

$$\begin{bmatrix} (\dot{\lambda}_1 - \dot{\lambda}_2)\sin\alpha \\ 0 \\ -(\dot{\lambda}_1 + \dot{\lambda}_2)\cos\alpha \end{bmatrix} + \begin{bmatrix} 0 & -w_3 & w_2 \\ w_3 & 0 & -w_1 \\ -w_2 & w_1 & 0 \end{bmatrix} \begin{bmatrix} (\lambda_1 - \lambda_2)\sin\alpha \\ 0 \\ -(\lambda_1 + \lambda_2)\cos\alpha \end{bmatrix} = \begin{pmatrix} u_x \\ u_y \\ u_z \end{pmatrix} \tag{3.10}$$

Here, $(u_x, u_y, u_z)^T$ are the collections of the terms that are not concerned with control inputs, thereby all known. To deal with this decoding equation, we divide (3.10) row-by-row, then we have

$$(\dot{\lambda}_1 - \dot{\lambda}_2)\sin\alpha - w_2(\lambda_1 + \lambda_2)\cos\alpha = u_x \tag{3.11}$$

$$w_3(\lambda_1 - \lambda_2)\sin\alpha + w_1(\lambda_1 + \lambda_2)\cos\alpha = u_y \tag{3.12}$$

$$-(\dot{\lambda}_1 + \dot{\lambda}_2)\cos\alpha - w_2(\lambda_1 - \lambda_2)\sin\alpha = u_z \tag{3.13}$$

Firstly, taking account of first and third row, we can combine (3.11) and (3.13) into matrix form as

$$\begin{bmatrix} \sin\alpha & -\sin\alpha \\ -\cos\alpha & -\cos\alpha \end{bmatrix} \begin{pmatrix} \dot{\lambda}_1 \\ \dot{\lambda}_2 \end{pmatrix} = \begin{bmatrix} u_x + w_2(\lambda_1 + \lambda_2)\cos\alpha \\ u_z + w_2(\lambda_1 - \lambda_2)\sin\alpha \end{bmatrix} \tag{3.14}$$

Here, note that w_2 is the angular velocity of current state. From (3.14), we can calculate thrust updates as,

$$\begin{aligned}\begin{pmatrix}\dot{\lambda}_1\\ \dot{\lambda}_2\end{pmatrix} &= \begin{bmatrix}\sin\alpha & -\sin\alpha\\ -\cos\alpha & -\cos\alpha\end{bmatrix}^{-1}\begin{bmatrix}u_x + w_2(\lambda_1+\lambda_2)\cos\alpha\\ u_z + w_2(\lambda_1-\lambda_2)\sin\alpha\end{bmatrix}\\ &= \begin{bmatrix}(u_x + w_2(\lambda_1+\lambda_2)\cos\alpha)/(2\sin\alpha) - (u_z + w_2(\lambda_1-\lambda_2)\sin\alpha)/(2\cos\alpha)\\ -(u_x + w_2(\lambda_1+\lambda_2)\cos\alpha)/(2\sin\alpha) - (u_z + w_2(\lambda_1-\lambda_2)\sin\alpha)/(2\cos\alpha)\end{bmatrix}\end{aligned} \tag{3.15}$$

Finally, we can calculate control input $\lambda_{1,2}$ by integrating (3.15).

Now let's consider the second row (3.12). This equation is not a *fact*, but rather a condition that should be satisfied. To make (3.12) to be satisfied, we backstep once again by using PD control as following.

$$\dot{\rho} = \dot{u}_y - \kappa(\rho - u_y) \tag{3.16}$$

where we define ρ as,

$$\rho := w_3(\lambda_1 - \lambda_2)\sin\alpha + w_1(\lambda_1+\lambda_2)\cos\alpha$$

Then, it can be guaranteed that $\rho \to u_y$, which results in equation (3.12) to be satisfied. Rewriting (3.16), after some manipulation, we get

$$\begin{bmatrix}(\lambda_1+\lambda_2)\cos\alpha & (\lambda_1-\lambda_2)\sin\alpha\end{bmatrix}\begin{pmatrix}\dot{w}_1^d\\ \dot{w}_3^d\end{pmatrix} = \bar{U} \tag{3.17}$$

where $\bar{U}$ stands for all the other terms except the left hand side (LHS) terms, which is indeed

$$\begin{aligned}\bar{U} := \dot{u}_y - \kappa[w_3(\lambda_1-\lambda_2)\sin\alpha + w_1(\lambda_1+\lambda_2)\cos\alpha - u_y]\\ - w_3(\dot{\lambda}_1-\dot{\lambda}_2)\sin\alpha - w_1(\dot{\lambda}_1+\dot{\lambda}_2)\cos\alpha\end{aligned}$$

Here, all terms in $\bar{U}$ is known since we already acquired $\dot{\lambda}_{1,2}$ in (3.15). Now we can design $\dot{w}_1^d$ and $\dot{w}_3^d$ as we want within the constraint of (3.17). Note that we have one more redundancy of choosing $\dot{w}_2^d$ which is pitch motion of the system. This redundancy is arisen from the increased actuation DOFs and can be utilized for generating any desired pitch motion independent with translational motion.

Then, we design attitude controller using $\dot{w}^d := [\dot{w}_1^d, \dot{w}_2^d, \dot{w}_3^d]^T$ which determined above, as

$$\tau = w \times Jw + J[\dot{w}^d - k_{att}(w - \int \dot{w}^d dt)] \tag{3.18}$$

where $k_{att} > 0$ is constant gain. Finally, we can calculate control command (i.e. thrust forces f_{ij}) from $\Lambda := (\lambda_1, \lambda_2, \tau) \in \Re^5$ using

$$\Lambda = \Sigma_\alpha \mathbf{f}_{ij} \tag{3.19}$$

Here, we recalled (2.7) and $\Sigma_\alpha \in \Re^{5\times 8}$ is thrust relationship we defined in Sec. 2.3.

3.2 Positive Thrust Constraint

Since most of the commercial BLDC motors can rotate in one-way, i.e. clockwise (CW) or counter-clockwise (CCW) as we connect the wires initially and propellers have its own pitch direction, thrust generated from the rotor has a mechanical constraint that should be *positive*. For example, a motor combined with counter-clockwised pitch propeller should rotate in CCW to generate proper air flow which ultimately results in reaction thrust force. See Fig. 3.1. So it need to be guaranteed that thrusts as a control input command have to be all positive values.

To ensure positiveness of thrusts, we exploit the redundancy of thrust-relationship (2.7). Since $\Sigma_\alpha \in \Re^{5\times 8}$ has null space of rank 3, we can use this redundancy for assuring positive thrust constraint. For this, we design an optimization as

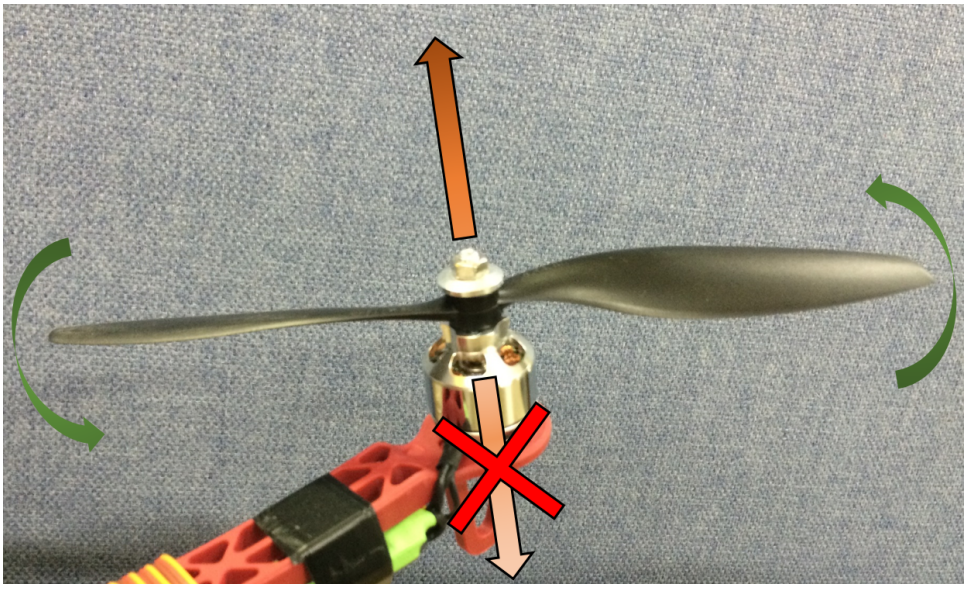

FIGURE 3.1: Positiveness of thrust

$$\begin{aligned} \min_{\mathbf{f}_{ij}} \quad & \|\mathbf{f}_{ij}^T \mathbf{f}_{ij}\| \\ \text{subj. to} \quad & \Lambda = \Sigma_\alpha \mathbf{f}_{ij} \\ & f_{ij} \geq 0 \end{aligned} \tag{3.20}$$

Here, minimizing objective function $\|\mathbf{f}_{ij}^T \mathbf{f}_{ij}\|$ means that choosing thrusts as similar to each other as possible. This implies that every thrusts are close to each other so that avoiding too big/small inputs, while satisfying the constraints. Equality constraint stands for the control and inequality constraint represents

the positiveness of thrusts.

For the most of the usual cases, the solution of this optimization (3.20) exists, but on the other hand, there may be some cases or trajectories, e.g. extreme flight maneuver, that equality and inequality constraints bring about conflict each other. Further consideration about this problem will be treated in the future research.

Chapter 4

Simulation

4.1 Simulation Scheme

For the asymmetrically coupled quadrotor UAVs system, we conducted simulations validating the theory in Sec. 3 and the capability of decoupling translation and rotation. Visual studio® C++ environment was used for the simulations and analysis was conducted with MATLAB®.

Simulation is structured as represented in Fig. 4.1. It is composed with 3 parts: controller part, dynamic simulation part, and graphic display part. Each of them is made up with individual loop thread and they exchange informations simultaneously.

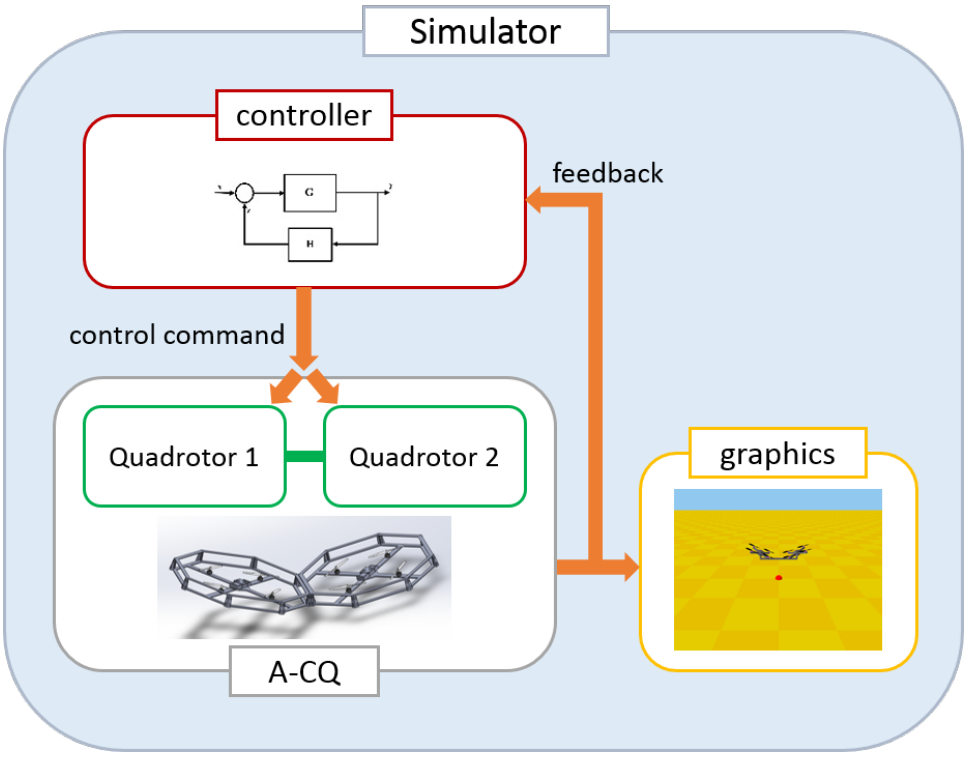

FIGURE 4.1: Simulation structure

In controller loop, the control which we designed in Sec. 3 is formulated with the state feedback from the dynamic simulation loop. Controller loop runs at 1 kHz and sends the control commands f_{ij} to each quadrotor in dynamic simulation thread. Dynamic simulation loop works as virtual asymmetrically coupled quadrotor UAVs system. It contains the dynamics and thrust relationship defined in Sec. 2, and the update rate is 1 kHz. From the controller thread, it gets the control commands of 8 motors and updates the state according to the dynamics.

And then the output state is transferred to both graphics loop and controller loop. In graphics loop, it displays the state of asymmetrically coupled quadrotor UAVs system visually using OpenGL (Open source Graphics Library)[29]. Graphics loop is updated at 50 Hz to show how the system is working to the users via display monitor. And finally, the state information from the dynamic simulation loop is provided to the controller loop to calculate the next step control commands.

4.2 Simulation Results

With the simulation scheme referred above, we performed various simulations to validate the theory and to demonstrate the features of the asymmetrically coupled quadrotor UAVs system. The system parameters and control gains we used in the simulation are listed in Table. 4.1.

TABLE 4.1: Parameters/gains used in simulation

α	20 deg	m	2 kg	η	4.0
l	0.118 m	b	3.6	γ	1.0
r	0.239 m	k	1.5	κ	6.0
k_τ	0.0136	ϵ	0.9	k_{att}	12.0

4.2.1 Trajectory tracking

Firstly, the simulation validating the controller designed in Sec. 3 is performed. Main issue is to follow the desired trajectory while positive thrust constraint is complied. Fig. 4.2 and 4.3 show the trajectory tracking performance of the system.

We set the desired trajectory as circle in x- and y-axis, combined with relatively slow oscillation along z-axis. Even with some initial position error, the system follows the desired trajectory soon and the error norm decreases to zero exponentially.

Here, we also see the plot of angular velocity w where quite different aspect than single quadrotor UAV is seen. In Fig. 4.4, you can see that only w_1, i.e. roll motion, is acting and w_2, w_3 are constantly zero. For single quadrotor UAV

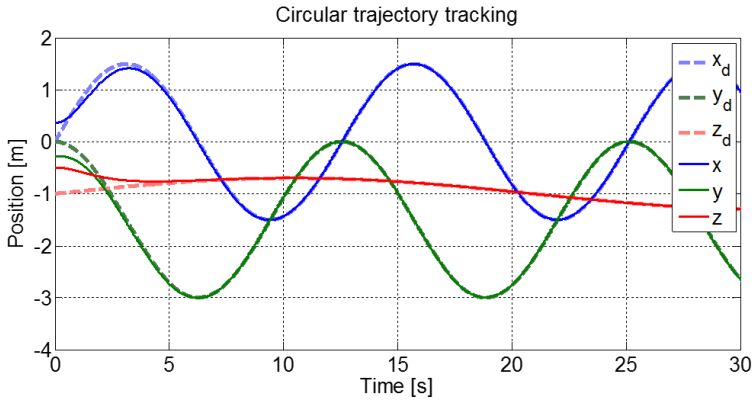

FIGURE 4.2: Trajectory tracking plot for circular trajectory

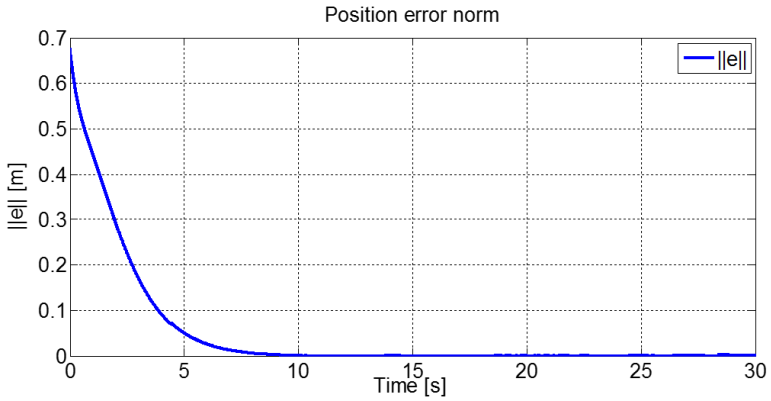

FIGURE 4.3: Position error plot for circular trajectory

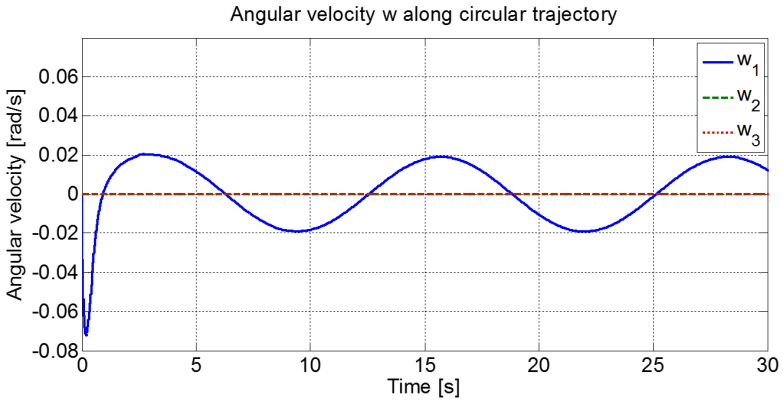

FIGURE 4.4: Angular velocity plot for circular trajectory

case, both w_1 and w_2 should change during circular trajectory tracking. This difference is from increased actuation of the asymmetrically coupled quadrotor UAVs system, thus we get additional degree of freedom to control where we used it to set w_2 to be zero during the flight, that is regulating pitch motion. This will be addressed deeper in the next simulation.

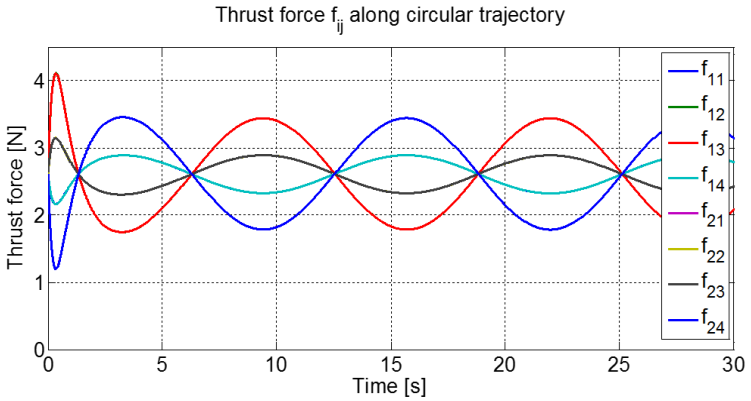

FIGURE 4.5: Thrust force plot for circular trajectory

Also, we can see that all thrusts are positive along the circular trajectory flight in Fig. 4.5. Therefore, we can conclude that the controller works properly and the system shows different motion than single quadrotor UAV.

4.2.2 Translation along x-axis without rotation

Unlikely to single conventional quadrotor UAV, proposed asymmetrically coupled quadrotor UAVs system has capability of decoupling translation and rotation. To reveal this feature, we conducted the simulation of translation along x-axis without rotation case. Fig. 4.6 shows the simulation snapshots of translation in x-axis. The desired trajectory is designed to be sinusoidal motion in x-direction while other components are kept constant. Desired trajectory and the tracking performance is plotted in Fig. 4.7.

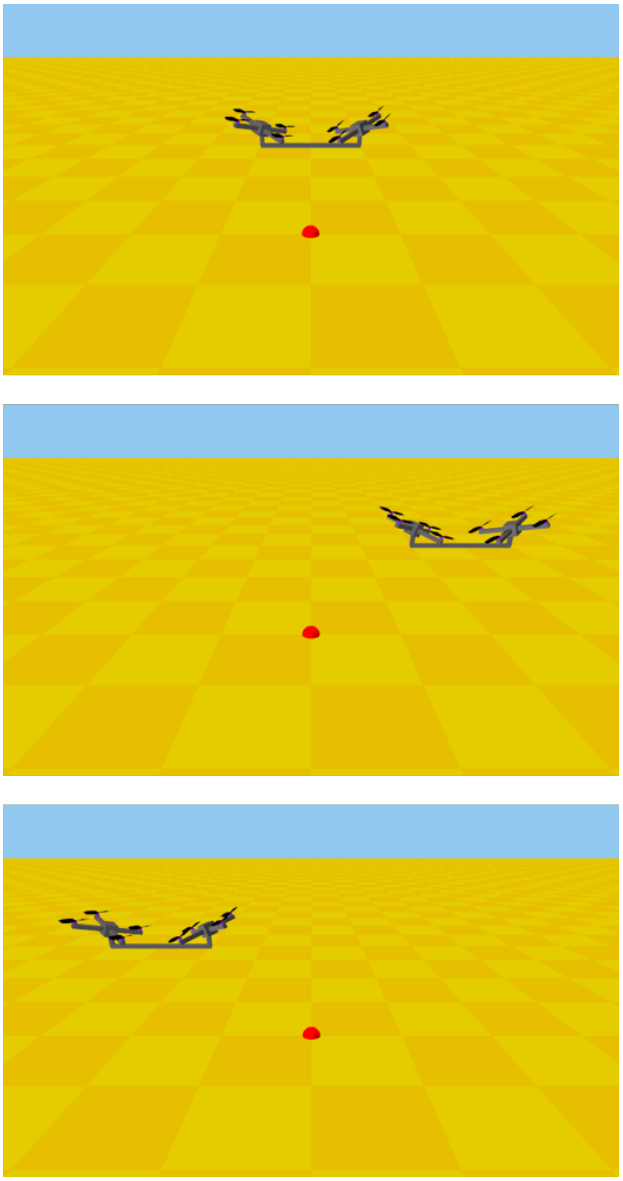

FIGURE 4.6: Simulation snapshot for x-axis trajectory

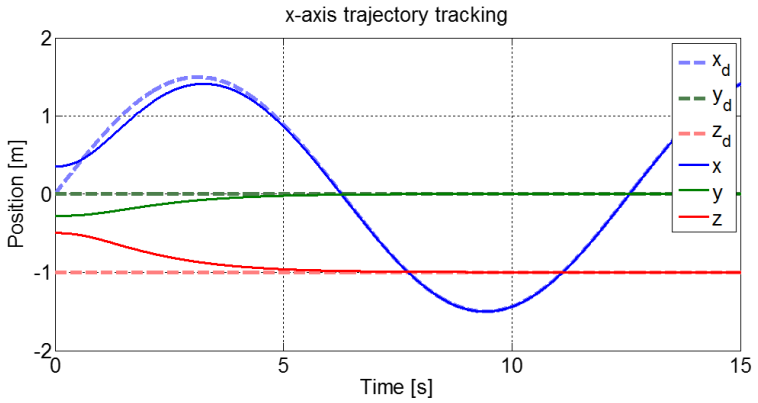

FIGURE 4.7: Trajectory tracking plot for x-axis trajectory

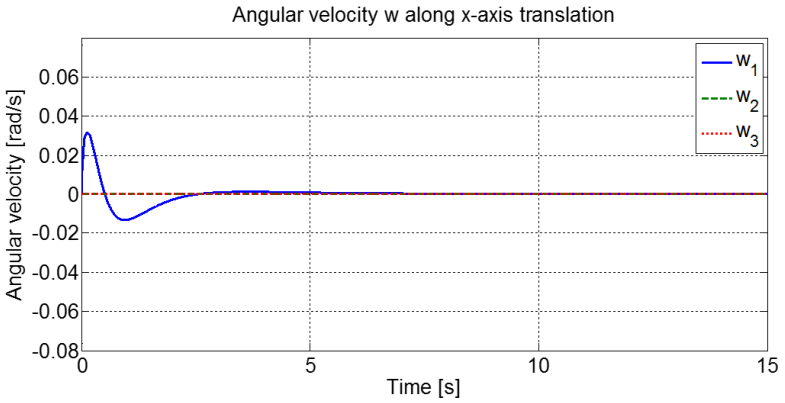

FIGURE 4.8: Angular velocity plot for x-axis trajectory

We stressed that the advantage of this system is increased actuation, which enables decoupling of translation and rotation motion. This can be easily demonstrated by this simulation as shown in Fig. 4.8. Except for the transient phase, there is no rotational motion generated while translation along x-axis. This means

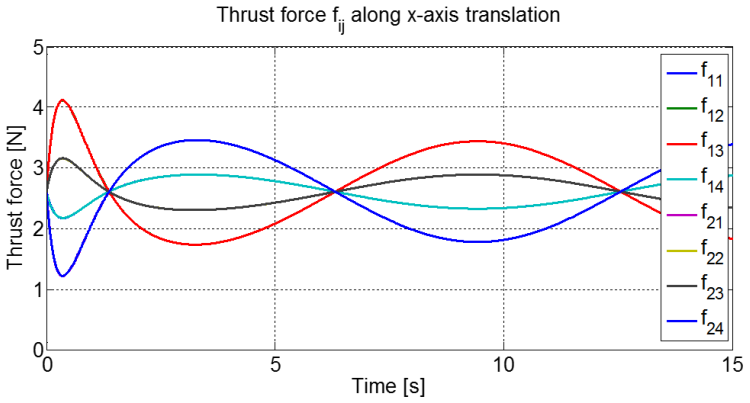

FIGURE 4.9: Thrust force plot for x-axis trajectory

that this system can move sideways without tilting itself showing that translation and rotation are independent each other. The way how this can be possible is using thrust vectoring referred earlier in Sec. 2.1. Compared to single quadrotor UAV which can generate thrust only in z-axis of body frame (thus tilting is inevitable for moving), this coupled system can generate horizontal force by combining asymmetric 8 thrust forces. That is, it changes the combination of 8 thrust forces to make side-way translational motion while maintaining the attitude as it is. This feature is desirable for many manipulation tasks which needs parallel translation of the platform and the tool. One example is shown in Sec. 4.2.5. Also in this case, all the thrust forces are positive complying the constraint as well. See Fig. 4.9.

4.2.3 Rotation without translation

On the other hand, since the system can decouple translation and rotation, we can also generate rotation without translation motion. Fig. 4.10 shows the simulation snapshot of rotation along y-axis (i.e. pitch motion) while keeping itself at the stationary position. On the contrary, in single conventional quadrotor UAV case, this is inherently impossible because translational movement occurs even with small amount of tilt. But for asymmetrically coupled quadrotor UAVs system, this can be accomplished by changing the combination of 8 thrust forces to generate only vertical net thrust, i.e. hovering at set-point, while making torque in pitch-direction.

To demonstrate this, we fix the desired trajectory as a set-point and modified $\dot{w}_2^d$ to make the pitch motion. Changing $\dot{w}_2^d$ whatever we want is possible within

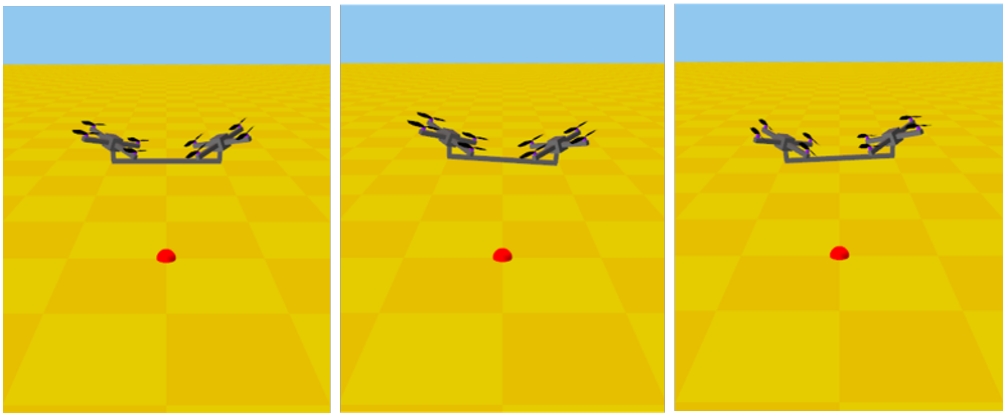

FIGURE 4.10: Simulation snapshot for rotation at set-point

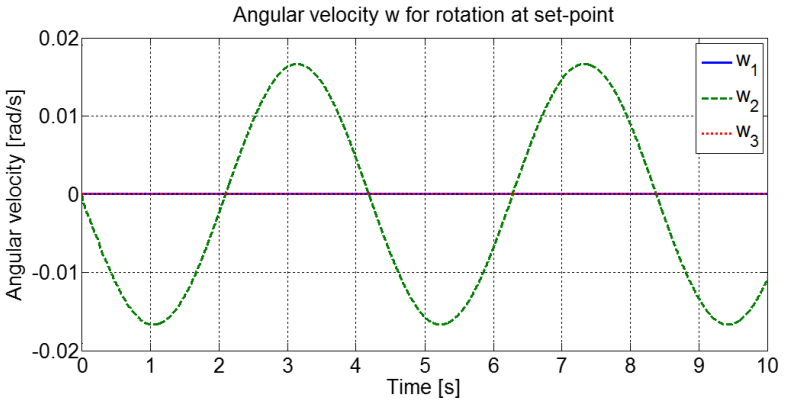

FIGURE 4.11: Angular velocity plot for rotation at set-point

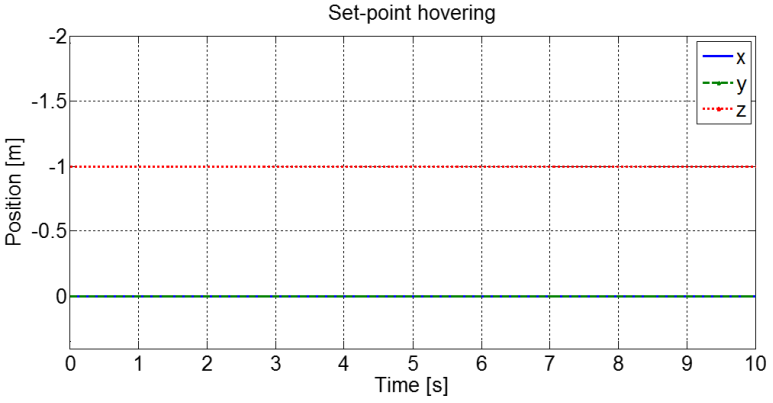

FIGURE 4.12: Keeping set-point position (0, 0, -1) while rotating

the range of that positive thrust constraint is not violated. Through Fig. 4.11 to 4.12, we can see that w_2 is acting (i.e. rotating in pitch angle) while keeping its position at set-point, e.g. $(0, 0, -1)m$ in this simulation, as mentioned.

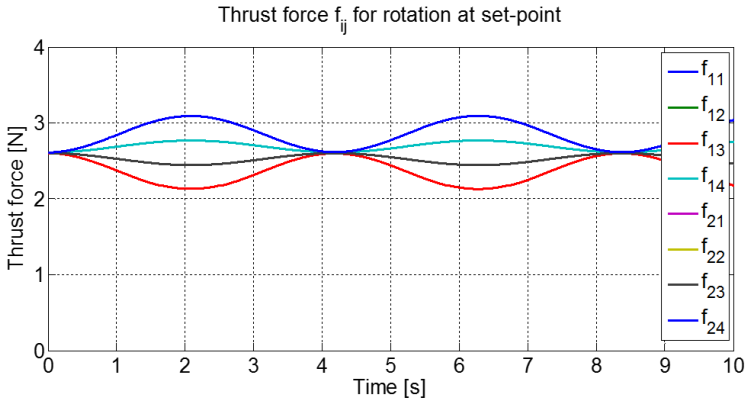

FIGURE 4.13: Thrust force plot for rotation at set-point

This feature is also useful for real manipulation tasks such as screwing, fastening the belt, or turning the handle, to name a few. Of course, again, all the thrust forces are positive as in Fig. 4.13.

4.2.4 Combination case

Moreover, not only for suppressing the other of translation or rotation as in Sec. 4.2.2 and Sec. 4.2.3 case, but controlling both independently is also possible. That is, we can make the system follow the desired trajectory while rotating itself as we want. This ability is common in ground vehicles, e.g. excavator, backhoe, or crane, however it is fairly rare for aerial manipulation since aerial vehicles don't have the ground to retain its posture. Therefore this ability can expand the versatility of the asymmetrically coupled quadrotor UAVs system for many complex tasks.

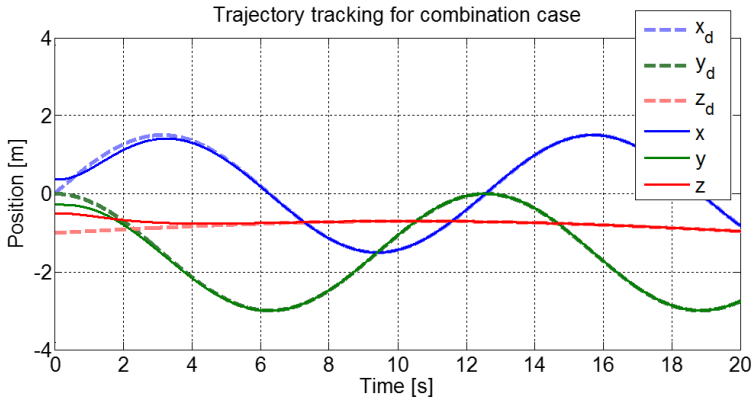

FIGURE 4.14: Trajectory tracking plot for combination case

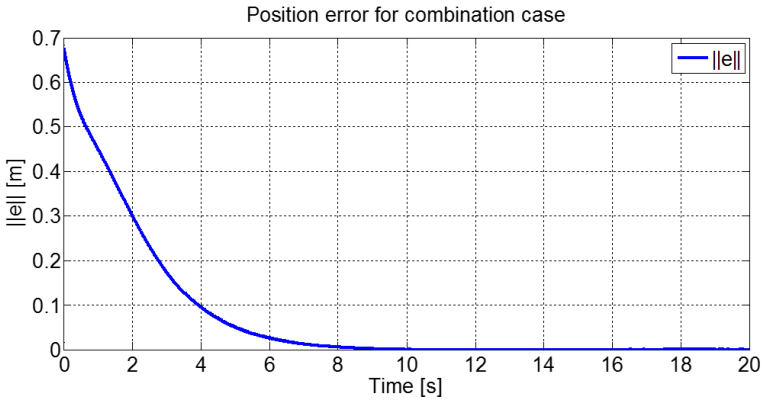

FIGURE 4.15: Position error plot for combination case

The desired trajectory and rotation motion are assigned same with each individual simulation case before. So the system follows the circular trajectory while tilting itself regardless of translational motion. Fig. 4.14 and 4.15 shows nice tracking performance similar with Sec. 4.2.1. Meanwhile, angular velocity w is

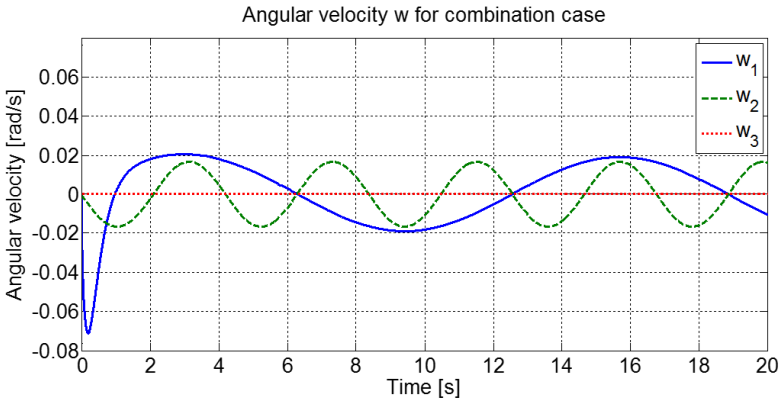

FIGURE 4.16: Angular velocity plot for combination case

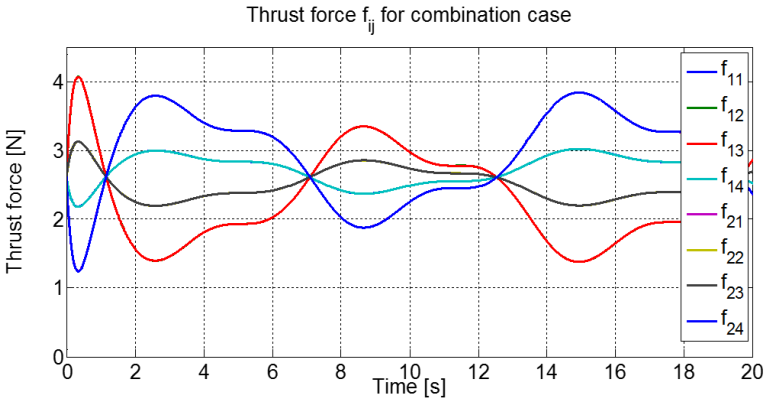

FIGURE 4.17: Thrust force plot for combination case

shown as Fig. 4.16. Here note that w_1 is acting because the asymmetrically coupled quadrotor UAVs system is still under-actuated in the sense of roll motion. The pitch motion w_2, however, shows irrelevant behavior with translational motion, only following the user-defined motion. Like the preceding, Fig. 4.17 shows that positiveness of thrust forces is guaranteed.

Still, under-actuation remaining along y-axis (i.e. roll motion) is quite distracting. But we can naturally bring to conclusion that fully-actuated system can be constructed by combining more than three quadrotor UAVs asymmetrically. Along with this idea, modularizing the system to widen its potential expandability will be interesting future research topic.

4.2.5 Tool operation example

Until now, we have shown the capability of decoupling translation and rotation of asymmetrically coupled quadrotor UAVs. Exploiting this feature, we expect that this system is suitable for real useful tasks such as tool operation and aerial manipulation. As one example, here, we demonstrate a simple scenario of tool operation which is pushing an object on the table. Fig. 4.18 shows the snapshots of the simulation. Asymmetrically coupled quadrotor UAVs system combined with a tool, is initially far away from the table, and soon come to near the object. Then, the tool-tip and the object get contacted and because of the friction, external force is injected to the system.

To deal with this external force, we exploit the admittance control similar to [30]. So the dynamics of the reference trajectory $x_r \in \Re^3$ can be written as

$$\tilde{M}(\ddot{x}_d - \ddot{x}_r) + \tilde{B}(\dot{x}_d - \dot{x}_r) + \tilde{K}(x_d - x_r) = -F_e \tag{4.1}$$

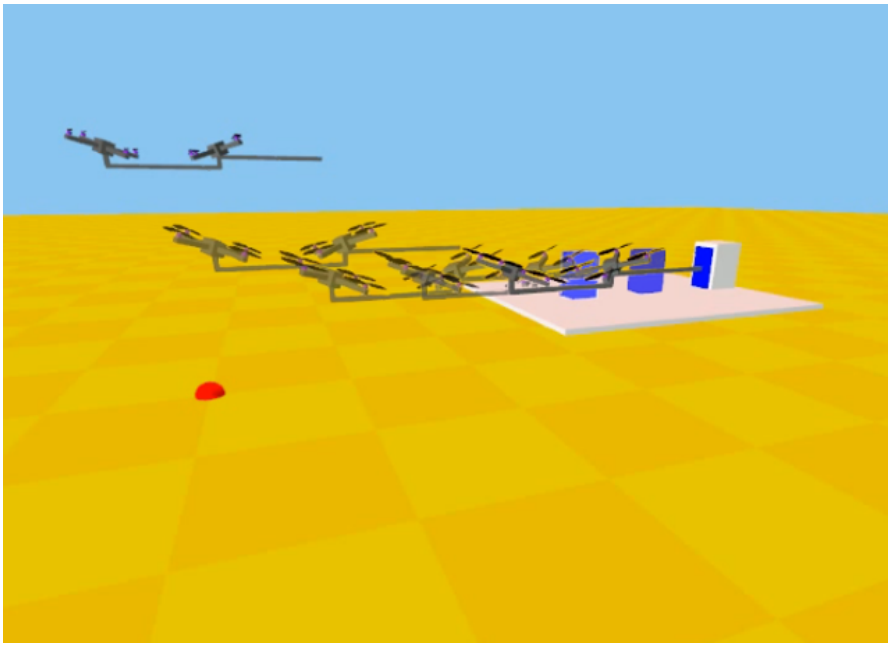

FIGURE 4.18: Simulation snapshot for tool operation

where $\tilde{M}, \tilde{B}, \tilde{K}$ are apparent inertia, damping, and stiffness, respectively, $x_d \in \Re^3$ is user-defined desired trajectory, and $F_e \in \Re^3$ stands for external force which, here, we assumed to be known from the force sensor. Following (4.1), the reference trajectory is modified by the external force so that works as the desired trajectory in the control (3.1). Using admittance control, we can achieve both trajectory tracking and compliance with the environment. [30]

In Fig. 4.19, it is shown that the trajectory tracking of the system for $x \rightarrow x_r$ works properly. Here, note that after contact with the object (near 7 sec),

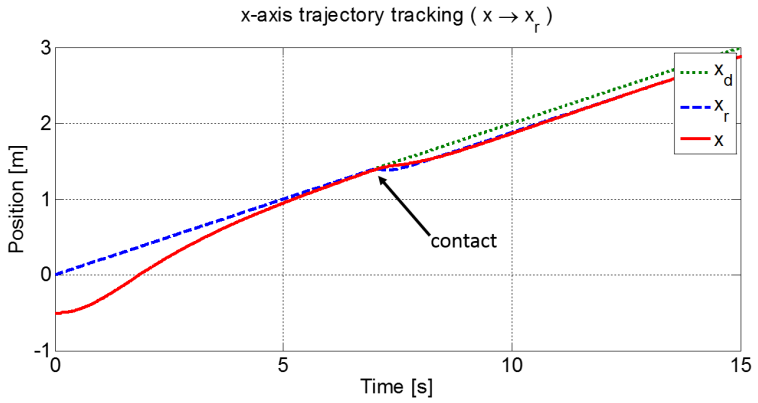

FIGURE 4.19: Trajectory tracking plot $x \rightarrow x_r$ for tool operation

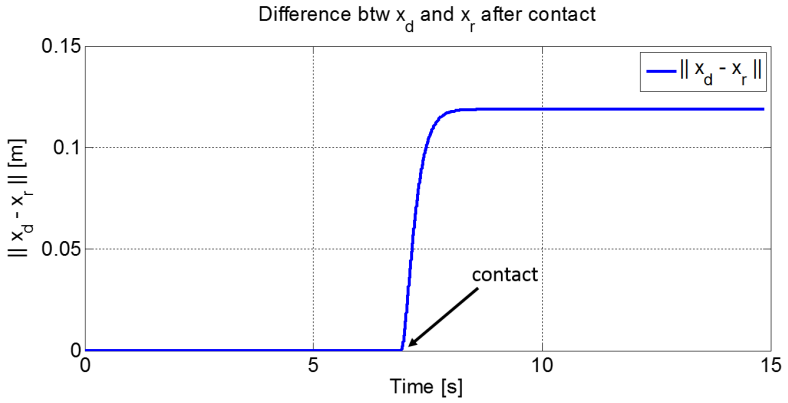

FIGURE 4.20: Difference between desired trajectory x_d and reference trajectory x_r along contact

the reference trajectory x_r has been changed due to external force so that the compliant pushing can be possible, see Fig. 4.20.

As we mentioned earilier, from the additional actuation DOF of this system, the tool operation can be done without any inclination of the tool or the platform,

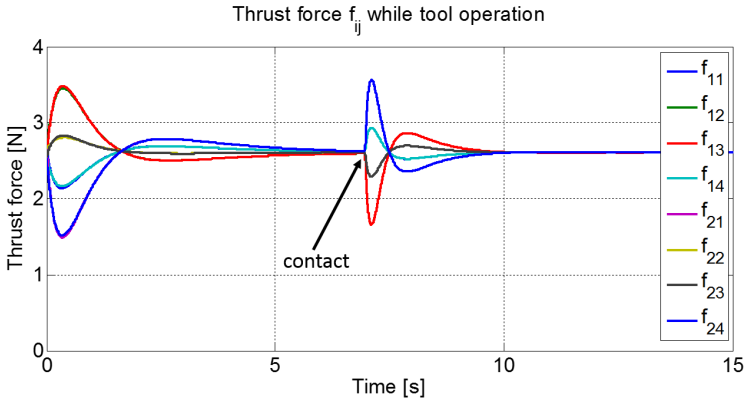

FIGURE 4.21: Thrust force plot for tool operation

which can be seen from the snapshot in Fig. 4.18. This feature allows us to design easier controller and is practical for various real world tasks. Also, even though there are contact and external force from the object, all thrust forces are maintained to positive values as in Fig. 4.21.

This example is just a very simple case to show one of the application of this system, however you can arrive to the conclusion that most of the aerial manipulation tasks can be conducted relatively easier with this asymmetrically coupled quadrotor UAVs system. Also, precise tool-tip control, force control with force estimation, or demonstration of some other applications will be considered in near future.

Chapter 5

Conclusion and Future Work

5.1 Conclusion

Throughout this thesis, we introduce a novel system which is asymmetrically coupled quadrotor UAVs. This system is composed with two conventional quadrotor UAVs that are rigidly coupled each other asymmetrically with coupling angle α. By combining two quadrotors inclined, this system has advantages in actuation DOFs, i.e. 5 actuations compared to 4 actuations for single quadrotor UAV case, as well as increased payload. This increased actuation allows us to decouple translation and rotation in a ceratin direction (e.g. coupled direction; x-axis in this paper). Utilizing this feature, the proposed system has capability to generate desired translational and rotational motion separately. Consequently, this system

is more versatile than single conventional quadrotor UAV, thus expecting to be useful for real tasks.

We first describe the design concept of asymmetrically coupled quadrotor UAVs, and model the dynamics of the system along with the kinematic relationship between total thrust and each thrust forces from the rotors. This thrust relationship is exploited throughout the control decoding part. Then we design controller for trajectory tracking of center of mass where we used backstepping control technique to deal with under-actuation problem. Also optimization is considered to optimize the thrust input under the constraint which is positiveness of thrust forces, that is all the thrust forces generated from the rotors should be positive due to its hardware limitation. Finally, various simulations are performed to illustrate the features of the proposed system and demonstrate the theory.

5.2 Future Work

The proposed asymmetrically coupled quadrotor UAVs system is a first step for milestone of modular quadrotor UAVs system. That is, this thesis does not confine the system to two quadrotor UAVs case, rather it is encourged to be extended to arbitrary number of modular quadrotor UAVs to reconfigure each other, namely *transformer* system. Combining three or more quadrotors as a modular platform can be an extension of this system that widely opening its potential, such as unlimited expandablity, fully-actuated system, and versatility

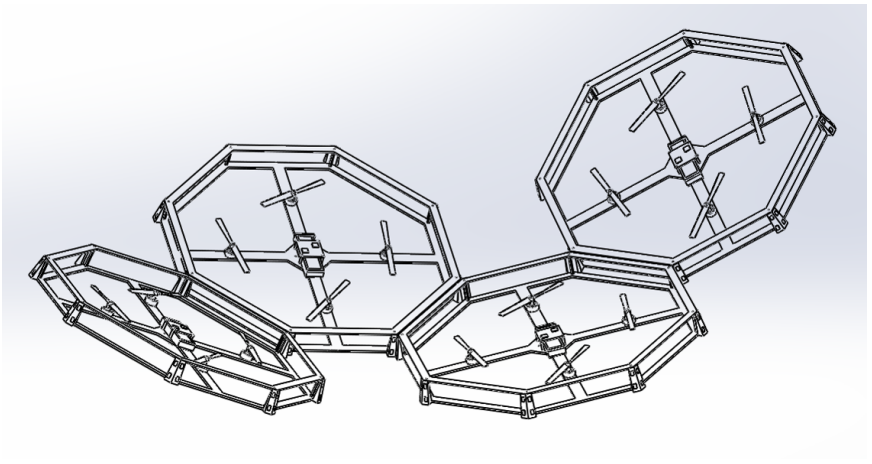

FIGURE 5.1: Concept design of modular quadrotor UAVs system

for real tasks. There are a number of future research topics related to this system and some possible topics are: 1) Design of airborne joint/disjoint mechanism for transformation; 2) Extension to arbitrary number of modular quadrotor UAVs; 3) Application to real useful tasks, e.g. aerial tool operation or aerial manipulation, etc.

Bibliography

[1] V. Kumar and N. Michael. Opportunities and challenges with autonomous micro aerial vehicles. *The International Journal of Robotics Research*, 31 (11):1279–1291, 2012.

[2] R. Mahony, V. Kumar, and P. Corke. Multirotor aerial vehicles: Modeling, estimation, and control of quadrotor. *Robotics & Automation Magazine, IEEE*, 19(3):20–32, 2012.

[3] K. Valavanis and G. J. Vachtsevanos. *Handbook of Unmanned Aerial Vehicles*. Springer, 2011.

[4] K. Nonami, F. Kendoul, S. Suzuki, W. Wang, and D. Nakazawa. *Autonomous Flying Robots: Unmanned Aerial Vehicles and Micro Aerial Vehicles*. Springer, 2010.

[5] D. J. Lee, C. Ha, and Z. Zuo. Backstepping control of quadrotor-type uavs and its application to teleoperation over the internet. In *Intelligent Autonomous Systems 12*, pages 217–225. Springer, 2013.

[6] H-N. Nguyen and D. J. Lee. Hybrid force/motion control and internal dynamics of quadrotors for tool operation. In *Intelligent Robots and Systems (IROS), 2013 IEEE/RSJ International Conference on*, pages 3458–3464. IEEE, 2013.

[7] H. Yang and D. J. Lee. Dynamics and control of quadrotor with robotic manipulator. In *Robotics and Automation (ICRA), 2014 IEEE International Conference on*, pages 5544–5549. IEEE, 2014.

[8] N. Michael, J. Fink, and V. Kumar. Cooperative manipulation and transportation with aerial robots. *Autonomous Robots*, 30(1):73–86, 2011.

[9] D. Mellinger, M. Shomin, N. Michael, and V. Kumar. Cooperative grasping and transport using multiple quadrotors. In *Distributed autonomous robotic systems*, pages 545–558. Springer, 2013.

[10] C. Pozna. Modular robots design concepts and research directions. In *Intelligent Systems and Informatics, 2007. SISY 2007. 5th International Symposium on*, pages 113–118. IEEE, 2007.

[11] R. Naldi, F. Forte, and L. Marconi. A class of modular aerial robots. In *Decision and Control and European Control Conference (CDC-ECC), 2011 50th IEEE Conference on*, pages 3584–3589. IEEE, 2011.

[12] T. Hamel, R. Mahony, R. Lozano, and J. Ostrowski. Dynamic modelling and configuration stabilization for an x4-flyer. *a a*, 1(2):3, 2002.

[13] M. D. Hua, T. Hamel, P. Morin, and C. Samson. A control approach for thrust-propelled underactuated vehicles and its application to vtol drones. *IEEE Transactions on Automatic Control*, 54(8):1837–1853, 2009.

[14] S. Bouabdallah and R. Siegwart. Full control of a quadrotor. In *Intelligent robots and systems, 2007. IROS 2007. IEEE/RSJ international conference on*, pages 153–158. IEEE, 2007.

[15] K. Sreenath, T. Lee, and V. Kumar. Geometric control and differential flatness of a quadrotor uav with a cable-suspended load. In *Decision and Control (CDC), 2013 IEEE 52nd Annual Conference on*, pages 2269–2274. IEEE, 2013.

[16] Q. Lindsey, D. Mellinger, and V. Kumar. Construction with quadrotor teams. *Autonomous Robots*, 33(3):323–336, 2012.

[17] J. Thomas, J. Polin, K. Sreenath, and V. Kumar. Avian-inspired grasping for quadrotor micro uavs. In *ASME 2013 International Design Engineering Technical Conferences and Computers and Information in Engineering Conference*, pages V06AT07A014–V06AT07A014. American Society of Mechanical Engineers, 2013.

[18] M. Ryll, H. H. Bulthoff, and P. R. Giordano. Modeling and control of a quadrotor uav with tilting propellers. In *Robotics and Automation (ICRA), 2012 IEEE International Conference on*, pages 4606–4613. IEEE, 2012.

[19] M. Ryll, H. H. Bulthoff, and P. R. Giordano. First flight tests for a quadrotor uav with tilting propellers. In *Robotics and Automation (ICRA), 2013 IEEE International Conference on*, pages 295–302. IEEE, 2013.

[20] P. Segui-Gasco, Y. Al-Rihani, H-S. Shin, and A. Savvaris. A novel actuation concept for a multi rotor uav. *Journal of Intelligent & Robotic Systems*, 74 (1-2):173–191, 2014.

[21] B. Michini, J. Redding, N. K. Ure, M. Cutler, and J. P. How. Design and flight testing of an autonomous variable-pitch quadrotor. In *Robotics and Automation (ICRA), 2011 IEEE International Conference on*, pages 2978–2979. IEEE, 2011.

[22] M. Cutler and J. P. How. Actuator constrained trajectory generation and control for variable-pitch quadrotors. In *AIAA Guidance, Navigation, and Control Conference (GNC),(Minneapolis, Minnesota)*, 2012.

[23] D. J. Lee. Distributed backstepping control of multiple thrust-propelled vehicles on a balanced graph. *Automatica*, 48(11):2971–2977, 2012.

[24] R. Oung and R. D'Andrea. The distributed flight array: Design, implementation, and analysis of a modular vertical take-off and landing vehicle. *The International Journal of Robotics Research*, 2013.

[25] R. Naldi, A. Ricco, A. Serrani, and L. Marconi. A modular aerial vehicle with redundant actuation. In *Intelligent Robots and Systems (IROS), 2013 IEEE/RSJ International Conference on*, pages 1393–1398. IEEE, 2013.

[26] C. Ha, Z. Zuo, F. B. Choi, and D. J. Lee. Passivity-based adaptive backstepping control of quadrotor-type uavs. *Robotics and Autonomous Systems*, 2014.

[27] H. K. Khalil. *Nonlinear systems*, volume 3. Prentice hall Upper Saddle River, 2002.

[28] R. Mahony and T. Hamel. Robust trajectory tracking for a scale model autonomous helicopter. *International Journal of Robust and Nonlinear Control*, 14(12):1035–1059, 2004.

[29] Open source graphics library. `https://opengl.org/`.

[30] F. Augugliaro and R. D'Andrea. Admittance control for physical human-quadrocopter interaction. In *Control Conference (ECC), 2013 European*, pages 1805–1810. IEEE, 2013.

요 약

본 논문에서는 두 대의 쿼드로터 무인비행로봇을 비스듬히 결합한 새로운 시스템을 제시한다. 본 시스템은 기존의 한 대의 쿼드로터가 가지는 부족구동(under-actuation)적인 측면과 낮은 적재하중의 문제를 극복하는 장점을 가진다. 즉, 기존에 쿼드로터가 4개의 구동 자유도를 갖는데 반해 본 시스템은 5개의 구동 자유도를 가져 한 차원의 제어가 추가로 가능하며, 이는 두 쿼드로터가 결합된 축 방향으로의 피치 (pitch) 동작에 대한 자유도로 활용할 수 있다. 이러한 특성은 공중 도구조작 (aerial tool operation) 등과 같은 실제 임무를 수행할 때 매우 유용하게 적용 가능하다. 제시된 비스듬히 결합한 쿼드로터 무인비행로봇 시스템에 대해 동역학 및 추력 관계식을 모델링하고, 궤적 추적 (trajectory tracking)을 위해 백스텝핑 제어기법을 활용한 제어를 설계하였다. 또한, 각 로터에서의 추력들이 항상 양의 값을 가져야하는 제약조건을 만족시키기 위한 최적화 기법을 제시하였다. 다양한 시뮬레이션을 통해 본 시스템과 제어기를 검증하였고 그 결과를 제시하였다.

주요어: Quadrotor UAV, Backstepping control, Under-actuation
학번: *2013-20721*